Neuron
Article

Postsynaptic Decoding of Neural Activity: eEF2 as a Biochemical Sensor Coupling Miniature Synaptic Transmission to Local Protein Synthesis

Michael A. Sutton,[1,3] Anne M. Taylor,[1] Hiroshi T. Ito,[1] Anh Pham,[1] and Erin M. Schuman[1,2,*]
[1] Division of Biology 114-96
[2] Howard Hughes Medical Institute
California Institute of Technology, Pasadena, CA 91125, USA
[3] Present address: Molecular and Behavioral Neuroscience Institute and Department of Molecular and Integrative Physiology, 5067 BSRB, University of Michigan, Ann Arbor, MI 48109-2200, USA.
*Correspondence: schumane@its.caltech.edu
DOI 10.1016/j.neuron.2007.07.030

SUMMARY

Activity-dependent regulation of dendritic protein synthesis is critical for enduring changes in synaptic function, but how the unique features of distinct activity patterns are decoded by the dendritic translation machinery remains poorly understood. Here, we identify eukaryotic elongation factor-2 (eEF2), which catalyzes ribosomal translocation during protein synthesis, as a biochemical sensor in dendrites that is specifically and locally tuned to the quality of neurotransmission. We show that intrinsic action potential (AP)-mediated network activity in cultured hippocampal neurons maintains eEF2 in a relatively dephosphorylated (active) state, whereas spontaneous neurotransmitter release (i.e., miniature neurotransmission) strongly promotes the phosphorylation (and inactivation) of eEF2. The regulation of eEF2 phosphorylation is responsive to bidirectional changes in miniature neurotransmission and is controlled locally in dendrites. Finally, direct spatially controlled inhibition of eEF2 phosphorylation induces local translational activation, suggesting that eEF2 is a biochemical sensor that couples miniature synaptic events to local translational suppression in neuronal dendrites.

INTRODUCTION

Recent work has implicated local dendritic protein synthesis in many enduring forms of synaptic plasticity, such as long-term potentiation and long-term depression (e.g., Kang and Schuman, 1996; Huber et al., 2000; Bradshaw et al., 2003), although the means by which synaptic activity is coupled to the protein synthetic machinery in dendrites remains poorly understood. The fact that these forms of synaptic modification require different patterns of synaptic activity for their induction raises the question of how the local translational machinery decodes these unique activity patterns. Here, we explore this issue in the context of endogenous levels of two qualitatively distinct forms of synaptic transmission: (1) action potential (AP)-triggered release of neurotransmitter and (2) miniature synaptic transmission (minis) mediated by spontaneous, AP-independent neurotransmitter release (Fatt and Katz, 1952). Previous results have shown that these two forms of neurotransmission regulate local translation in opposite directions—blocking APs alone inhibits, whereas blocking both APs and minis stimulates, dendritic protein synthesis (Sutton et al., 2004, 2006). These observations suggest that neuronal dendrites possess a biochemical sensor that is specifically tuned to miniature synaptic transmission and capable of engaging the dendritic translation machinery.

In principle, this sensor could be represented by a general signaling pathway that is broadly coupled to protein translation, or alternatively, it could be a signal that is dedicated to the regulation of protein translation machinery itself. One candidate in the latter category is eukaryotic elongation factor-2 (eEF2) and its associated kinase, Ca^{2+}/calmodulin-dependent protein kinase III (CAMKIII; Nairn and Palfrey, 1987), now known as eEF2 kinase. eEF2 catalyzes ribosomal translocation during polypeptide elongation. Phosphorylation of eEF2 at Thr56 strongly inhibits its activity, thereby inhibiting protein synthesis (Ryazanov et al., 1988; Redpath et al., 1993). In addition, eEF2 phosphorylation is known to be stimulated by strong activation of ionotropic glutamate receptors (GluRs; Marin et al., 1997; Scheetz et al., 2000; Chotiner et al., 2003) and can be regulated in isolated synaptic biochemical fractions (Scheetz et al., 2000; Carroll et al., 2004). These findings raise the possibility that eEF2 phosphorylation might serve to couple particular patterns of synaptic input to local translational suppression in neuronal dendrites.

Here, we demonstrate that eEF2 is a biochemical sensor tuned to ongoing levels of miniature synaptic transmission in hippocampal neurons. Similar to the regulation of dendritic protein synthesis, basal AP-dependent

and miniature transmission regulate eEF2 phosphorylation in opposite directions, with miniature events positively associated with the amount of eEF2 that is in its phosphorylated (translationally inactive) state. The regulation of eEF2 phosphorylation by miniature transmission is bidirectional—blocking minis markedly reduces, whereas enhancing minis stimulates, eEF2 phosphorylation. Moreover, miniature events regulate eEF2 locally in dendrites, and this regulation in turn inhibits dendritic translation in a spatially specific fashion. Taken together, our results suggest that eEF2 is a local sensor of miniature synaptic activity in dendrites that serves to couple this form of neurotransmission to local translational suppression.

RESULTS

Miniature Synaptic Events Inhibit Dendritic Protein Synthesis Locally

Previous work has shown that AP-dependent and miniature synaptic transmission regulate dendritic protein synthesis in opposite directions—blocking APs with tetrodotoxin (TTX) inhibits dendritic translation, whereas blocking miniature events stimulates dendritic protein synthesis (Sutton et al., 2004, 2006). Bath application of TTX, however, blocks both presynaptic and postsynaptic APs. To confine the effects of TTX to presynaptic neurons, we used a microfluidic chamber (Taylor et al., 2005) in which presynaptic or postsynaptic neurons can be fluidically isolated (Figures 1A and 1B). Application of TTX to the presynaptic compartment blocked spiking of presynaptic neurons but did not prevent postsynaptic neurons from spiking (Figure 1C). We then followed the presynaptic TTX application with postsynaptic APV to examine the effects of blocking the NMDA receptor (NMDAR)-mediated component of miniature neurotransmission on dendritic protein synthesis. Time-lapse imaging of dendrites expressing a fluorescent translation reporter (Figure 1D; Aakalu et al., 2001) revealed that, whereas control dendrites treated with TTX alone exhibited a small decline in fluorescence over time, inhibition of NMDAR minis resulted in an increase in dendritic protein synthesis (Figures 1E and 1F). These results indicate that the translational activation accompanying mini blockade is evident during selective elimination of presynaptic APs.

To examine the spatial specificity of this translational regulation, we used a dual micropipette delivery system to locally perfuse different dendritic regions of conventionally cultured neurons expressing the dendritic protein synthesis reporter. Pyramidal-like hippocampal neurons in culture were perfused continuously in HEPES-buffered saline (HBS) containing TTX (1 μM) to block all AP-induced evoked neurotransmission. After a baseline image series was taken, dendritic segments were locally perfused with TTX plus a cocktail of GluR antagonists (the AMPA receptor [AMPAR] antagonist, CNQX [40 μM] and the NMDAR antagonist APV [60 μM]), and changes in the rate of reporter synthesis over time were monitored. A fluorescent dye (Alexa 568) was included in the delivery perfusate to monitor the perfusion area throughout the experiment. We compared changes in reporter expression in the treated dendritic segment with those of other segments of the same dendrite outside the perfused area both prior to and following local perfusion. As shown in Figures 2A–2D, we found that the change in reporter expression in the treated area was initially comparable with that of other segments of the same dendrite (at t = 0 min), but following local mini blockade, perfused areas demonstrated a progressive increase in reporter expression over the next 100 min (Figures 2B–2D). Restricted perfusion of vehicle alone (Figures 2E and 2F) was ineffective in altering local reporter synthesis, and the stimulation of local protein synthesis by mini blockade was completely prevented by bath application of the protein synthesis inhibitor anisomycin (40 μM; Figure 2F). These results indicate that local blockade of excitatory miniature neurotransmission enhances dendritic protein synthesis in a spatially specific fashion.

eEF2: A Biochemical Sensor Uniquely Regulated by Miniature Neurotransmission

How do postsynaptic neurons distinguish minis from AP-driven input, and how is this distinction conveyed to the translation machinery in dendrites? To begin to address this question, we first examined the regulation of two signaling pathways strongly linked to translational control in most eukaryotic systems: the ERK-MAPK and PI3 kinase pathways (for reviews, see Holland, 2004; Ruggero and Sonenberg, 2005). We measured the phosphorylation status of ERK isoforms and Akt, a well-known downstream target of the PI3 kinase pathway, under conditions of AP block alone (with TTX) or block of both APs and excitatory miniature neurotransmission (TTX+CNQX+APV). Whereas the phosphorylation of Akt was unaltered by either manipulation, the phosphorylation (and presumably activity) of both ERK isoforms (p42 and p44) exhibited strong activity sensitivity: phosphorylation was depressed by AP blockade (Figure 3A) and exhibited an even stronger depression when minis were also blocked. These results identify the ERK-MAPK signaling pathway as a system that is highly sensitive to levels of postsynaptic activity, but it does not appear differentially responsive to evoked and spontaneous neurotransmission.

We next examined if posttranslational regulation of eEF2 accompanies mini blockade. eEF2 catalyzes ribosomal translocation during polypeptide elongation, and phosphorylation of eEF2 near the N terminus (at Thr56) is known to strongly inhibit its activity in the elongation phase of protein synthesis (Ryazanov et al., 1988; Redpath et al., 1993). We found that unlike ERK phosphorylation, the regulation of eEF2 phosphorylation by AP-dependent and miniature neurotransmission was both qualitatively and quantitatively distinct. Relative to control, AP blockade alone induced significantly *greater* phosphorylation of eEF2 at Thr56, whereas additional blockade of miniature transmission produced significantly *diminished* levels of eEF2 phosphorylated at that site

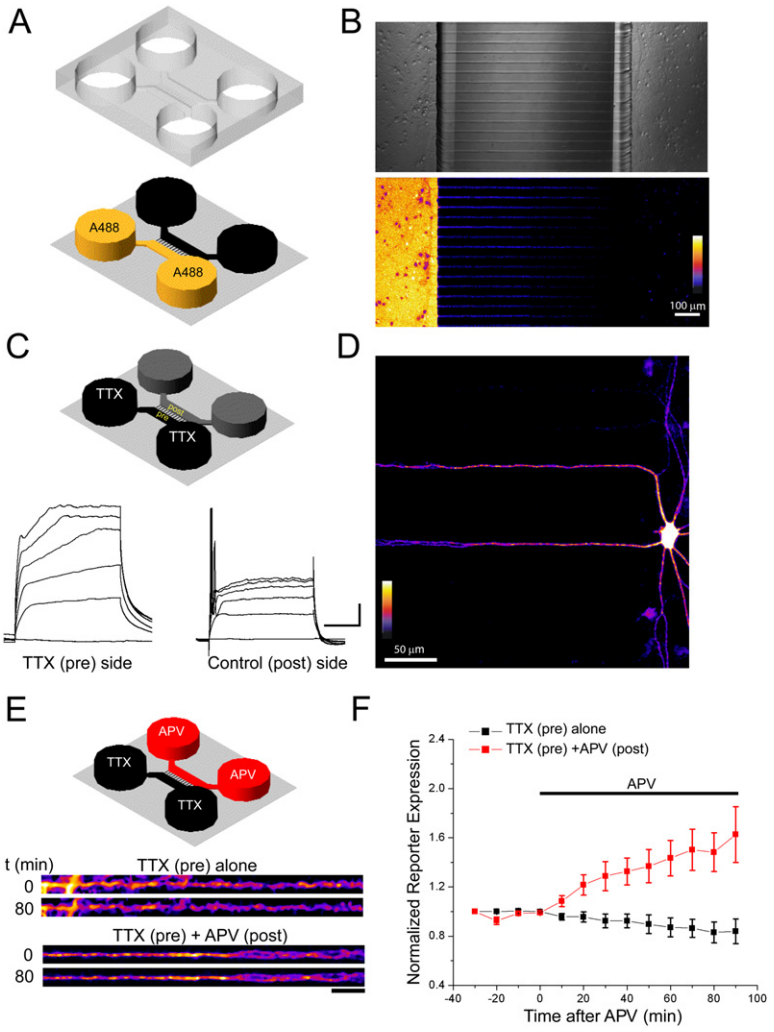

Figure 1. Selective Blockade of Presynaptic APs with Postsynaptic Block of NMDAR Minis Leads to an Enhancement of Dendritic Protein Synthesis

(A) Schematic of microfluidic culture chamber containing two (one "presynaptic" and one "postsynaptic") somatic compartments connected by microgrooves. A volume difference between the somatic compartments (~50 μl) established a pressure difference between them, allowing each chemical microenvironment to be isolated for several hours.

(B) DIC image of a microfluidic chamber; cell bodies are evident in both somatic compartments and axons and dendrites can be observed in the microgrooves. Addition of Alexa Fluor 488 (MW 570) to the presynaptic cell body compartment shows that the dye only extends partially into the proximal grooves and negligibly affects the dendritic or somatic region at the other end of the chamber after 3 hr of isolation. Alexa 488 fluorescence intensity is indicated by the color look-up table.

(C) TTX was added to the presynaptic somatic compartment. After 60 min, current-clamp recordings were obtained from cell bodies in either presynaptic or postsynaptic compartments. TTX addition blocked spiking in presynaptic neurons in response to current injection, but did not block spiking of postsynaptic neurons. Scale bar, 10mV, 100 ms. These data indicate that TTX acts selectively on presynaptic neurons in this experiment.

(D) Example of a neuron expressing the GFP translation reporter in the postsynaptic compartment. Dendrites extend into microgrooves where they come into contact with axons (not visible here); fluorescence intensity (reporter expression) is indicated by the color look-up table.

(E) Design of experiment. TTX (5 μM) (see Experimental Procedures) was added to the presynaptic compartment to block APs; 1–1.5 hr later, baseline images were taken every 10 min, then APV (250 μM) (see Experimental Procedures) was isolated to the postsynaptic compartment. In control experiments, TTX was isolated to the presynaptic compartment for the baseline images, then buffer (instead of APV) was added to the postsynaptic somatic side. Fluorescence images of dendrites expressing the GFP translation reporter were obtained before (t = 0 min) and after (t = 80 min) the addition of APV to block the NMDAR component of miniature excitatory synaptic events; fluorescence intensity as in (D). Scale bar, 20 μm. Inhibition of NMDAR minis led to an enhancement of dendritic translation, as compared with control (TTX alone)-treated dendrites.

(F) Ensemble average of all control (TTX alone, n = 3 experiments, five dendrites) and NMDAR mini block (TTX pre + APV post, n = 4 experiments, eight dendrites) experiments. Inhibition of NMDAR minis led to a significant and rapid enhancement of dendritic protein synthesis.

(Figure 3A). Total levels of eEF2 protein were not different between the groups, suggesting that minis regulate eEF2 phosphorylation posttranslationally. These results indicate that eEF2 phosphorylation is differentially tuned to AP-dependent and miniature synaptic transmission, and the direction of the changes are consistent with eEF2 playing a causal role in the local translational suppression mediated by excitatory miniature events.

Bidirectional Regulation of eEF2 Phosphorylation by Miniature Synaptic Transmission

If eEF2 is a sensor of miniature neurotransmission, then an increase in Thr56 phosphorylation should occur when miniature transmission is enhanced. To address this question, we used α-latrotoxin (α-LTX), which is known to stimulate the release of predocked synaptic vesicles from presynaptic terminals (e.g., Ceccarelli et al., 1973). In whole-cell voltage-clamp recordings (n = 8), we confirmed that a low concentration of α-LTX (100 pM; in combination with 0.1 mM $LaCl_3$ to prevent formation of α-LTX pores; Ashton et al., 2001) stimulates miniature release by approximately 1.5- to 2-fold (Figure 3B1; see also Sutton et al., 2004). We thus examined whether augmenting miniature neurotransmission enhances eEF2 phosphorylation during AP blockade. As shown in Figure 3B, treatment with TTX alone enhanced eEF2 phosphorylation

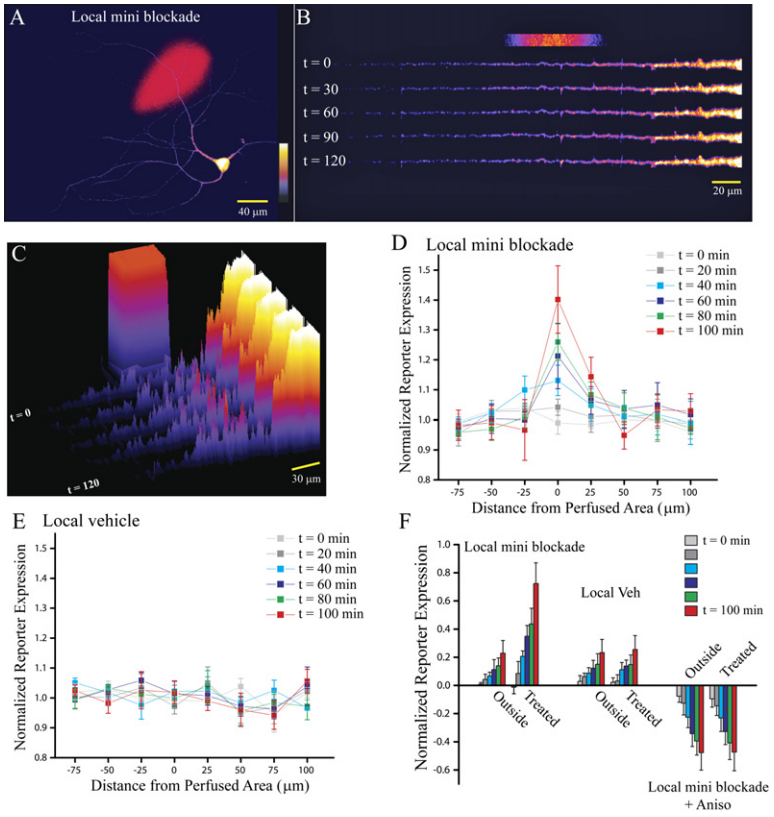

Figure 2. Blockade of Excitatory Minis Induces Local Translation in Dendrites

Example and summary of local perfusion experiments in cultured hippocampal neurons (>21 DIV) expressing a GFP-based fluorescent translation reporter (Aakalu et al., 2001). Neurons were globally treated with TTX (1 μM, bath applied) to block AP-dependent neurotransmission prior to spatially restricted perfusion of either a mini-blocking cocktail (the AMPAR antagonist CNQX [40 μM] plus the NMDAR antagonist APV [60 μM]; n = 10 dendrites from six cells) or vehicle as a control (n = 8 dendrites from four cells). In an additional set of experiments, local mini blockade was examined with protein synthesis blocked by bath application of anisomycin (40 μM; n = 10 dendrites from five cells).

(A–C) Example of an experiment in which prior bath application of TTX was followed by local perfusion of a mini-blocking cocktail for 120 min. (A) Shown is a neuron expressing the protein synthesis reporter, with superimposed perfusion area demarcated by Alexa 568 (present in the local perfusate in all experiments) fluorescence in red. (B) A time-lapse montage of the dendrite (straightened) from the cell shown in (A) from initiating local perfusion to 120 min later, at 30 min intervals; the perfusion area is marked in red above the dendrites. (C) 3D plot of fluorescence intensity in the same dendrite from t = 0–120 min, at 30 min intervals; relative fluorescence intensity (reporter expression) is indicated by the color and height of the pixels. A spatially specific and progressive increase in dendritic reporter expression in the treated area (indicated by color tower above t = 0) was evident after local disruption of miniature synaptic transmission.

(D and E) Summary data. Mean (±SEM) change in reporter expression with local mini blockade (D) or vehicle (E) in different segments of treated dendrites over time, relative to baseline (20 min prior to local perfusion), normalized to the average change in untreated dendritic segments. Whereas the rate of change in vehicle-treated segments closely matched that in untreated regions of the same dendrite at all time points, a progressive increase in reporter expression, relative to other areas of the same dendrite, was evident in segments treated locally with CNQX+APV.

(F) Mean (±SEM) change in reporter expression (relative to baseline) in untreated and treated segments of dendrites over time in the three conditions examined. Under anisomycin treatment, a progressive loss in reporter expression was observed over time due to the lack of protein synthesis; the rate of reporter loss in treated versus untreated dendritic segments was indistinguishable, indicating that local mini blockade does not alter local reporter degradation or accumulation.

relative to untreated controls, but additional treatment with α-LTX produced a significantly greater phosphorylation of eEF2 that was sustained for at least 60 min. In contrast, block of miniature synaptic transmission with GluR antagonists again produced significantly diminished levels of p-eEF2 relative to control. Importantly, the effect of α-LTX was lost when minis were blocked postsynaptically, indicating that its positive effects on eEF2 phosphorylation require the integrity of miniature neurotransmission. Taken together, these results indicate that the phosphorylation of eEF2 is bidirectionally regulated by miniature synaptic transmission.

The phosphorylation of eEF2 at Thr56 is catalyzed by eEF2 kinase, a Ca^{2+}/calmodulin-dependent protein kinase (Nairn and Palfrey, 1987). Since NMDARs, rather than AMPARs, are the principal source of activity-dependent Ca^{2+} influx at synapses, we next examined the role of these different receptor types in mediating eEF2 phosphorylation during miniature transmission (Figure 3C). We found that blocking only the NMDAR component of miniature neurotransmission (TTX+APV) was sufficient to inhibit eEF2 phosphorylation during AP blockade, and the additional blockade of AMPARs (TTX+CNQX+APV) did not significantly alter the magnitude of this effect. These results suggest that the regulation of eEF2 phosphorylation by minis is primarily downstream of NMDAR activation.

To further validate the role of NMDAR minis in regulating eEF2 phosphorylation, we examined whether blocking voltage-gated Ca^{2+} channels that support AP-triggered neurotransmitter release would also enhance eEF2 phosphorylation at Thr56. Similar to the effects of direct AP blockade (with TTX), neurons treated with antagonists to the Ca^{2+} channels associated with evoked transmission at hippocampal synapses (N-type channel blocker ω-conotoxin GVIA, 1 μM, and the P/Q-type blocker ω-agatoxin IVA, 200 nM; Wheeler et al., 1994) exhibited increased levels of p-eEF2 relative to untreated controls. As before,

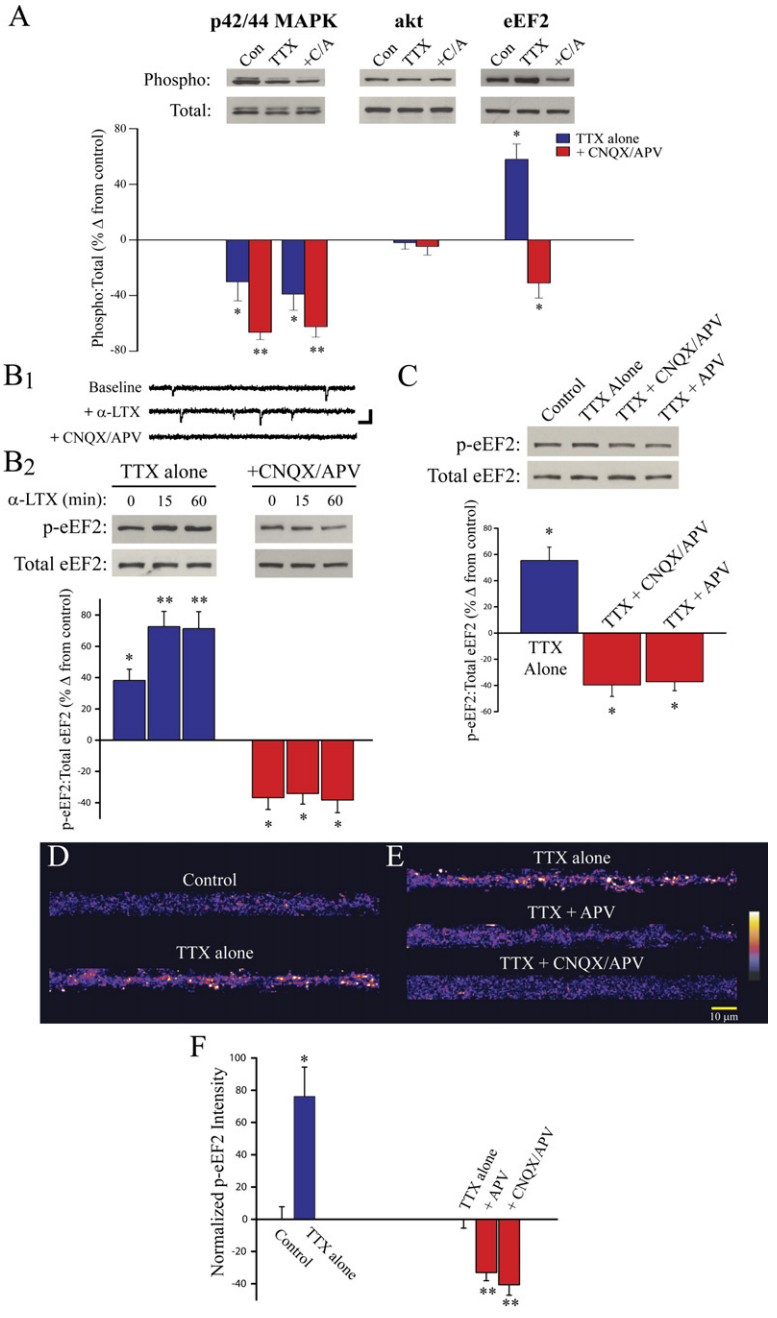

Figure 3. Bidirectional Regulation of eEF2 Phopshorylation by Miniature Synaptic Transmission

(A) To examine potential regulation of translation-relevant signaling pathways by miniature neurotransmission, neurons were either untreated (control) or treated with TTX (2 μM) for 12 hr with or without mini blockade (CNQX [40 μM] + APV [50 μM]) for the last 2 hr. Representative western blots (top) and summary data (below) using antibodies specific for dually phosphorylated (Thr202/Tyr204) and total p42/p44 MAPK, phosophorylated (Ser473) and total Akt, and phosphorylated (Thr56) and total eEF2 are shown. Whereas PI3 kinase signaling (using phosphorylated Akt as a downstream readout) was unaffected by either condition of activity blockade, p42/p44 MAP kinase signaling was strongly depressed by AP blockade alone, and even more so by the additional blockade of miniature neurotransmission (TTX+CNQX+APV). By contrast, eEF2 was regulated in opposite directions by AP versus mini blockade: TTX alone lead to significantly enhanced levels of p-eEF2 (the inactive form), whereas mini blockade lead to significantly diminished levels of p-eEF2 (i.e., a larger proportion of active eEF2). Data are from eight independent experiments.

(B) To examine if the regulation of eEF2 phosphorylation by minis is bidirectional, neurons were treated with TTX with or without mini blockade as in (A), and additionally challenged with α-latrotoxin (α-LTX; 100 pM) to stimulate miniature transmission. (B1) Representative whole-cell voltage-clamp recording demonstrating the frequency of mEPSCs in the same neuron in the presence of TTX alone (baseline), 10 min after addition of 100 pM α-LTX, and 5 min following addition of CNQX+APV. Scale bar, 100 ms, 10 pA. (B2) Stimulating miniature transmission with α-LTX significantly enhanced eEF2 phosphorylation; this effect required the integrity of miniature synaptic activity—mini blockade with CNQX+APV completely prevented the increase in p-eEF2 with α-LTX.

(C) Blockade of the NMDAR component of miniature neurotransmission alone (TTX+APV) produced comparable decreases in eEF2 phosphorylation to blocking both the AMPAR and NMDAR components, suggesting that the regulation of eEF2 by excitatory miniature transmission is primarily downstream of the NMDARs.

(D–F) To assess whether AP blockade enhances eEF2 phosphorylation in dendrites, neurons were either untreated (control, n = 33) or treated with TTX (2 μM) for 2.5 hr (n = 31) prior to fixation and labeling with an antibody specific for p-eEF2. To examine if miniature transmission promotes eEF2 phosphorylation in dendrites, neurons were treated with TTX (2 μM; 2.5 hr) either alone (n = 31) or coincident with APV (60 μM; n = 33) or CNQX (40 μM) + APV (n = 33) over the last 1.5 hr. (D and E) Representative straightened dendrites from untreated controls and each of the above treatment conditions; color look-up table indicates p-eEF2 immunofluorescence intensity. (F) Mean (±SEM) change in dendritic p-eEF2 intensity relative to average control (left) or average in TTX alone (right). TTX alone led to significantly elevated levels of p-eEF2 in dendrites; coincident mini blockade led to significantly diminished dendritic levels of p-eEF2.

For all panels, *p < 0.05 versus control; **p < 0.05 versus TTX alone.

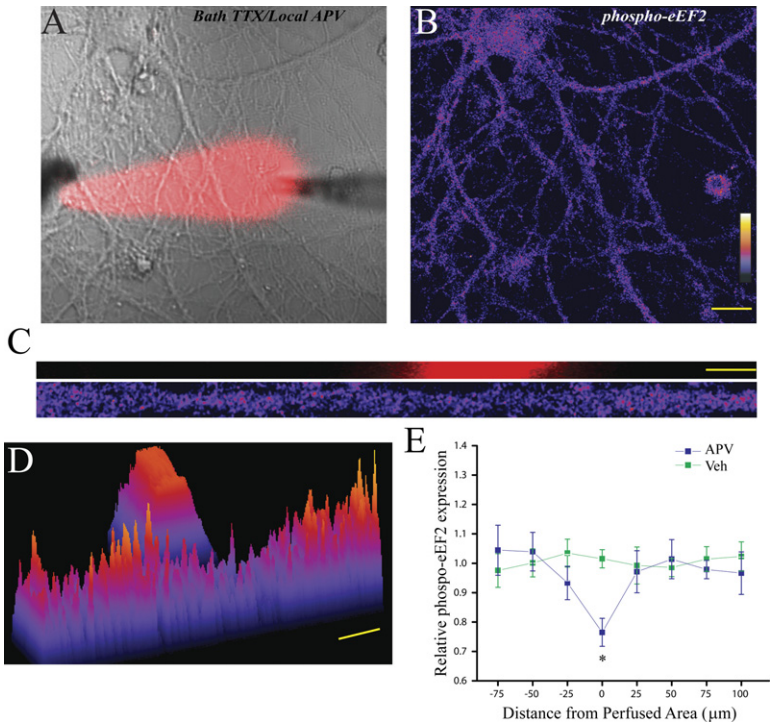

Figure 4. Spatially Restricted NMDAR Mini Blockade Produces a Local Decrease in eEF2 Phosphorylation

TTX (1 μM) was bath applied approximately 60 min prior to local perfusion of either TTX+APV (60 μM; n = 11 dendrites from six cells) or TTX+vehicle (n = 9 dendrites from five cells) for 60 min.

(A) DIC image showing neuron with local APV perfusion spot (red).

(B) p-eEF2 staining for the neuron shown in (A); intensity of p-eEF2 immunofluorescence given by color look-up table. Scale bar, 20 μm.

(C) Straightened dendrite from the cell shown in (A) and (B); the perfused area is also shown above the dendrite in red. Scale bar, 10 μm.

(D) 3D plot of relative p-eEF2 immunofluorescence for the dendrite shown in (C); perfusion spot is also indicated. Scale bar, 20 μm.

(E) Summary data. Mean (±SEM) relative p-eEF2 fluorescence intensity, normalized to the average nonzero pixel intensity outside the treated area. On the abscissa, positive and negative values indicate segments distal and proximal (toward), respectively, from the treated area. Local NMDAR mini blockade led to a significant (*$p < 0.05$) decrease in p-eEF2 expression in the treated region, whereas local perfusion of vehicle had no effect.

coincident blockade of NMDARs produced the opposite effect—significantly diminished levels of p-eEF2 (Figure S1 in the Supplemental Data available with this article online). Thus, the differential regulation of eEF2 phosphorylation by AP-dependent and miniature neurotransmission revealed in our earlier experiments is not strictly dependent on blocking APs per se, but rather on evoked neurotransmitter release.

Minis Regulate eEF2 Phosphorylation in Neuronal Dendrites

To further examine activity-dependent eEF2 phosphorylation, we stained neurons with an antibody specific for p-eEF2 (Marin et al., 1997) and examined the levels of p-eEF2 in the dendrites of neurons treated with AP blockade alone or a coincident blockade of miniature synaptic transmission (Figure 3D–3F). Similar to our biochemical experiments, neurons treated with TTX alone exhibited marked elevation of p-eEF2 in dendrites relative to untreated controls (Figure 3D). Coincident blockade of both AMPAR and NMDAR-dependent miniature neurotransmission (TTX+CNQX+APV) during TTX treatment strongly counteracted the increase in eEF2 phosphorylation observed with AP block alone. Again, this effect was primarily mediated by NMDARs, since selective blockade of NMDAR miniature neurotransmission (TTX+APV) largely accounted for the decrease in p-eEF2 levels in dendrites (Figures 3E and 3F). Together, these results demonstrate that ongoing miniature synaptic transmission, acting primarily through NMDAR activity, stimulates eEF2 phosphorylation in neuronal dendrites.

Minis Regulate eEF2 Phosphorylation Locally in Dendrites

We next asked whether minis can regulate eEF2 phosphorylation locally in dendrites. To address this, we blocked APs in the entire dish (by bath application of TTX) and then locally blocked NMDARs using restricted perfusion of APV. Post hoc immunostaining for p-eEF2 revealed that local blockade of NMDAR minis (for 60 min) resulted in a decrease in p-eEF2 in the treated area relative to adjacent dendritic segments (Figures 4A–4E), whereas local perfusion of vehicle alone had no effect on p-eEF2 expression (Figure 4E). Conversely, local enhancement of miniature synaptic transmission by spatially restricted delivery of α-LTX during global AP blockade produced the opposite effect—a specific increase in p-eEF2 levels in perfused dendritic segments relative to other dendritic segments (Figures 5A–5E). These effects on local p-eEF2 levels were not due to redistribution of eEF2 in dendrites, since the relative levels of total eEF2, independent of the phosphorylation state, were not altered by restricted perfusion of either APV or α-LTX (Figure 5F). Together, these results indicate that the phosphorylation of eEF2 at Thr56 is bidirectionally and locally regulated in neuronal dendrites by levels of miniature neurotransmission.

The Regulation of eEF2 Phosphorylation by Minis Locally Controls Translation in Dendrites

The above results indicate that ongoing miniature synaptic transmission potently regulates eEF2 phosphorylation, primarily via the activity of NMDARs. Given that this

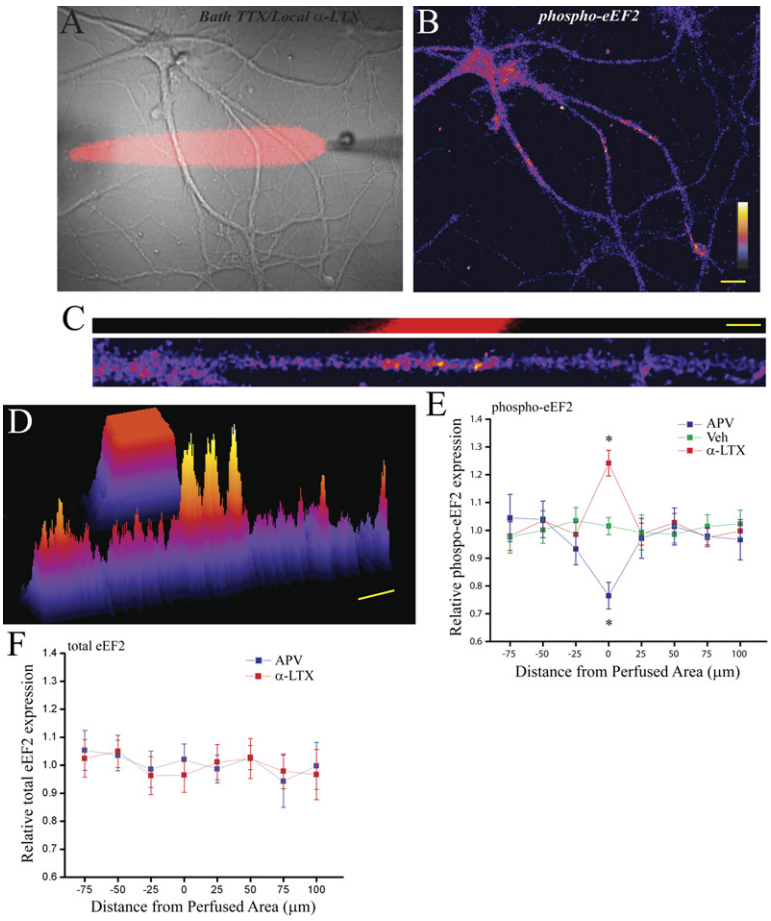

Figure 5. Local Enhancement of Miniature Transmission Stimulates eEF2 Phosphorylation

TTX (1 μM) + $LaCl_3$ (0.1 mM) was bath applied approximately 60 min prior to local perfusion of the same solution plus 500 pM α-LTX for an additional 45–60 min (n = 11 dendrites from five cells).

(A) DIC image showing neuron with local α-LTX perfusion spot (red).

(B) p-eEF2 staining for the neuron shown in (A); intensity of p-eEF2 immunofluorescence given by color look-up table. Scale bar, 20 μm.

(C) Straightened dendrite from the cell shown in (A) and (B); the perfused area is also shown above the dendrite in red. Scale bar, 10 μm.

(D) 3D plot of relative p-eEF2 immunofluorescence for the dendrite shown in (C). Scale bar, 20 μm.

(E) Summary data. Mean (±SEM) relative p-eEF2 fluorescence intensity, normalized to the average nonzero pixel intensity outside the treated area. On the abscissa, positive and negative values indicate segments distal and proximal (toward soma), respectively, from the treated area. Data for local APV and local vehicle groups are replotted from Figure 3 for comparison. Local enhancement of miniature neurotransmission led to a significant (*$p < 0.05$) increase in p-eEF2 expression in the treated region, indicating that the local regulation of eEF2 phosphorylation by minis is bidirectional.

(F) Summary data for experiments examining dendritic expression of total eEF2 (independent of phosphorylation state) after local perfusion with APV (n = 8 dendrites from four cells) or α-LTX (n = 9 dendrites from four cells). Data are expressed as in (E). Neither local APV nor local α-LTX altered overall expression of eEF2 in the treated area.

phosphorylation inhibits eEF2 function, we hypothesized that activation of eEF2 kinase by NMDAR minis contributes to the translational suppression that miniature events normally provide. If so, then inhibiting the kinase should be sufficient to stimulate translation. To address this question, we took advantage of two distinct eEF2 kinase inhibitors, rottlerin (Gschwendt et al., 1994) and NH125 (Arora et al., 2003), and examined their effect on protein synthesis (using the reporter described above) in dendrites when APs were blocked. After acquiring a baseline image in the presence of TTX alone, neurons were acutely challenged with either rottlerin (5 μM), NH125 (10 μM), or vehicle (TTX alone) and imaged 60 and 120 min later. While neurons maintained in TTX alone exhibited stable levels of reporter expression in distal dendrites, those acutely challenged with rottlerin or NH125 each exhibited marked increases in dendritic reporter expression over time (Figures 6A and 6B). To examine if these changes in reporter expression were due to enhanced protein synthesis, we repeated the same experiment in the presence of the protein synthesis inhibitor anisomycin (40 μM). Reporter expression in neurons treated with anisomycin diminished substantially over time, and importantly, the rate of reporter loss was nearly identical under the three conditions examined (Figures 6C and 6D). These results indicate that the increase in reporter expression observed after blocking eEF2 kinase is due to enhanced protein synthesis rather than other posttranslational factors (e.g., degradation).

Finally, since rottlerin is also known to inhibit PKCδ, we examined the effects of a PKC inhibitor, Bisindolylmaleimide I (Bis; 1 μM), at a concentration that effectively blocks this isoform. Unlike the effects of rottlerin or NH125, coincident administration of Bis during TTX did not alter dendritic reporter expression relative to TTX alone (mean ± SEM baseline at 120 min: TTX alone, 91.2% ± 14.6%; TTX + Bis, 88.6% ± 17.3%; n = 12 cells/group, nonsignificant). Thus, the enhanced rates of reporter synthesis observed with rottlerin and NH125 cannot be attributed to their effects on PKC.

Given that under conditions of intact miniature transmission, direct inhibition of eEF2 kinase stimulates dendritic protein synthesis, we next asked whether the local

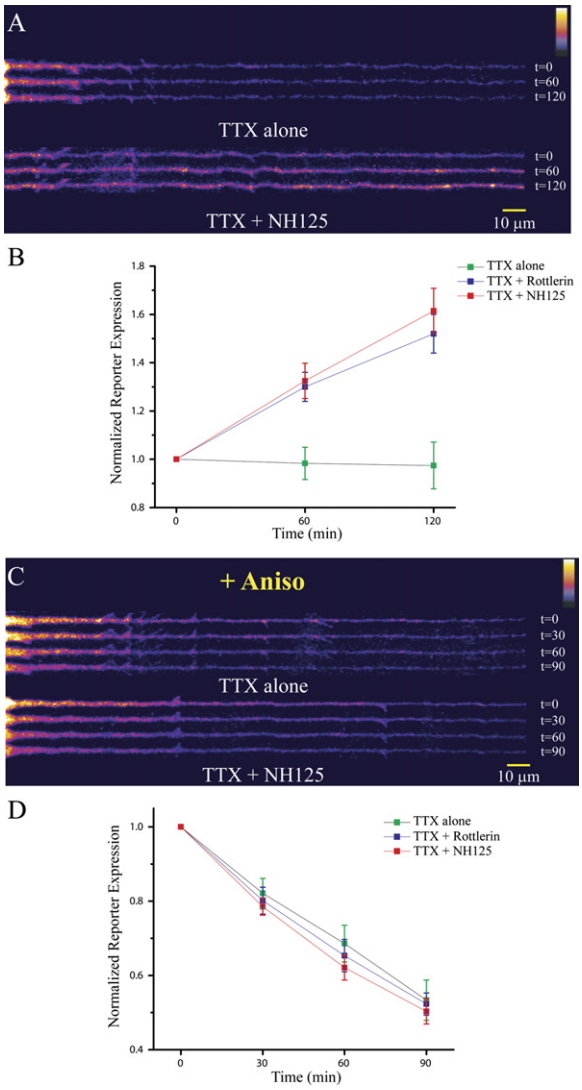

Figure 6. Inhibition of eEF2 Kinase during Miniature Transmission Drives Dendritic Protein Synthesis

Neurons (n = 16 cells/group) expressing the protein synthesis reporter were treated with TTX (2 μM) prior to imaging, and challenged with one of two distinct eEF2 kinase inhibitors—rottlerin (5 μM) or NH125 (10 μM)—immediately following acquisition of a baseline image (t = 0). A second set of experiments examined the same treatment conditions (n = 14 cells/group) in the presence of the protein synthesis inhibitor anisomycin (40 μM).

(A) A time-lapse montage of straightened dendrites from cells either maintained in TTX alone or acutely challenged with NH125.

(B) Mean (±SEM) reporter expression (relative to baseline) in the distal dendritic compartment (>125 μm from soma) for each of the three treatment conditions. Treatment with rottlerin or NH125 enhanced dendritic reporter expression, whereas expression remained stable in the presence of TTX alone.

(C) A time-lapse montage of straightened dendrites from cells treated as in (A), but in the presence of anisomycin.

(D) Mean (±SEM) reporter expression (relative to baseline) in distal dendrites in each of the three treatment conditions in the presence of anisomycin. Substantial decreases in reporter expression over time were evident with anisomycin treatment, but the rate of reporter turnover in the absence of protein synthesis was similar among treatment groups. Fluorescence intensity is indicated by the color look-up table in (C).

regulation of eEF2 phosphorylation by miniature neurotransmission is sufficient to provide spatially specific control of dendritic translation. After a baseline image series was acquired in the presence of bath-applied TTX, dendritic segments were locally perfused with TTX+NH125 to block eEF2 kinase in a spatially defined area. For locally treated dendrites, we compared changes in reporter expression in the treated dendritic segment with those of other dendritic segments outside the perfused area both prior to and 0–80 min following local perfusion of NH125. For dendrites that did not pass through the perfusion area (untreated), we compared changes in reporter expression in an area of identical size and distance from the cell soma as the treated dendrites from the same neurons. We found that the change in reporter expression in the treated area was initially comparable to that of other segments of the same dendrite (t = −20 to 0 min), but following local NH125 perfusion, treated areas demonstrated a progressive increase in reporter expression over the next 80 min (Figures 7A–7C). By contrast, no such differential effect was observed in untreated dendrites (Figure 7D) from the same neurons, and local perfusion of TTX alone also did not alter reporter synthesis locally (Figure 2E), indicating that the marked increase in local reporter expression was specifically due to NH125 treatment. These results thus indicate that eEF2 kinase activity not only exerts control over dendritic protein synthesis, but that it does so in a spatially limited manner.

DISCUSSION

We have demonstrated that eEF2 acts as a local biochemical sensor for miniature synaptic transmission, serving to couple this form of neurotransmission to local translational suppression in dendrites. Other studies have demonstrated a strong relationship between phosphorylation of eEF2 and translational suppression in cultured neurons (Marin et al., 1997), synaptic biochemical fractions (Scheetz et al., 2000), or hippocampal slices (Chotiner et al., 2003) in response to intense activation of ionotropic GluRs. Here, we find that eEF2 phosphorylation driven by miniature neurotransmission acts to constrain neuronal protein synthesis, working locally within intact neuronal dendrites to suppress translation in a spatially specific fashion. Interestingly, we have also found that intrinsic AP-dependent network activity in cultured hippocampal neurons maintains eEF2 in a relatively dephosphorylated (active) state, suggesting that basal levels of AP-dependent and miniature neurotransmission regulate eEF2 in opposite directions, similar to their opposing influences on dendritic protein synthesis (Sutton et al., 2004). Thus, while eEF2 phosphorylation is clearly engaged by intense increases in AP-triggered neurotransmission, its responsiveness to AP-dependent and miniature synaptic

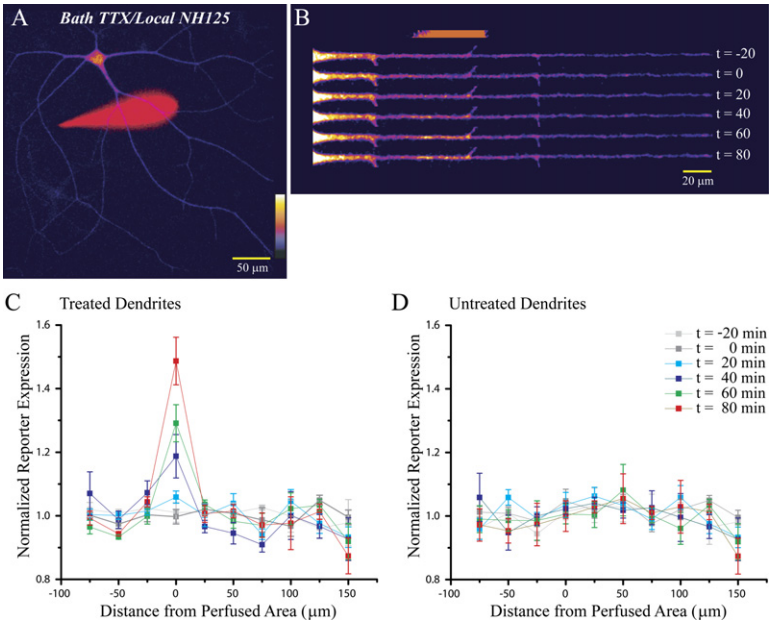

Figure 7. Spatially Restricted Blockade of eEF2 Kinase Stimulates Local Dendritic Protein Synthesis

Neurons expressing the translation reporter and treated with TTX (2 μM) were imaged before and after local perfusion with NH125 (10 μM; starting at t = 0).

(A) Shown is a neuron with superimposed perfusion area demarcated by Alexa 568 fluorescence in red.

(B) A time-lapse montage of a straightened dendrite from the cell shown in (A) from 20 min before to 80 min following local perfusion, at 20 min intervals; the perfusion area (in red) is also shown above the dendrites. Fluorescence intensity is indicated by the color look-up table in (A).

(C and D) Mean (±SEM) change in reporter expression in different segments of treated (C) or untreated (D) dendrites (n = 12 and 10 dendrites, respectively, from six cells) over time relative to baseline (40 min prior to local perfusion) normalized to the average change in the same dendrites outside the perfusion area. Dendrites from the same cells as in (C), but not passing through the perfusion area, were used for the analysis in (D); an area identical in size and distance from the soma (relative to the corresponding treated dendrite from the same neuron) was used for the "perfusion area" in (D). Spatially restricted blockade of eEF2 kinase induced local reporter synthesis in treated dendrites, whereas reporter expression in the same region of untreated dendrites remained consistent with the dendrite as a whole.

transmission is qualitatively distinct during periods of normal AP-triggered network activity.

eEF2 Is a Biochemical Sensor Tuned to Local Miniature Synaptic Transmission

In recent years, it has become clear that different activity-driven signaling pathways at synapses are capable of encoding particular features of the activity patterns that activate them. For example, CAMKII, a protein kinase strongly implicated in the induction of long-term potentiation (e.g., Malinow et al., 1989; Silva et al., 1992; Barria et al., 1997), is capable of decoding the frequency of Ca^{2+} oscillations in vitro (De Koninck and Schulman, 1998). Likewise, persistent activation of p42/p44 MAPK by membrane depolarization in cultured hippocampal neurons is critically dependent on spacing of individual stimuli (Wu et al., 2001). Our results indicate that p42/p44 MAPK is generally tuned to the absolute levels of synaptic activity, without specific responsiveness to the quality of neurotransmission (i.e., whether the activity derives from evoked or spontaneous release). By contrast, the activity-dependent phosphorylation status of eEF2 is critically dependent on relative levels of AP-dependent and miniature synaptic transmission. When AP-dependent transmission dominates, a sizeable amount of eEF2 is dephosphorylated. However, during AP blockade, when miniature neurotransmission dominates, a marked increase in eEF2 phosphorylation results. We have further shown that this eEF2 phosphorylation is specifically driven by miniature neurotransmission, since increasing (with α-LTX) or removing (with GluR antagonists) the impact of minis produces corresponding increases or decreases in eEF2 phosphorylation. Finally, using restricted perfusion techniques, we have shown that this bidirectional regulation of eEF2 phosphorylation by miniature neurotransmission is implemented in a spatially specific fashion. These results suggest that eEF2 phosphorylation is tuned to local levels of miniature synaptic transmission.

Unique Modes of Translational Inhibition Conferred by AMPAR and NMDAR Minis

Phosphorylation of eEF2 at Thr56 is catalyzed by a Ca^{2+}/calmodulin-dependent protein kinase (Nairn and Palfrey, 1987). Thus, the fact that minis regulate eEF2 phosphorylation primarily through NMDARs suggests a model in which the Ca^{2+} influx through the NMDAR engages this phosphorylation step directly, through activation of eEF2 kinase. In support of this notion, the open-channel NMDAR antagonist MK-801, when applied during AP blockade, also drives dendritic protein synthesis (data not shown), suggesting that ion flux through the NMDARs rather than glutamate binding is responsible for the translational suppression. Moreover, the characteristics of eEF2 kinase match well with the small currents generated by miniature release; for example, relative to CAMKII, eEF2 kinase is activated by >5-fold lower Ca^{2+} concentrations (Hughes et al., 1993) and exhibits approximately two orders of magnitude greater affinity for calmodulin (Mitsui et al., 1993). Thus, whereas CAMKII has been shown to effectively decode aspects of AP-triggered

neurotransmission such as input frequency (e.g., De Koninck and Schulman, 1998), eEF2 kinase seems optimized for decoding asynchronous activity on a dramatically different scale of sensitivity.

Previous studies have indicated that AMPAR and NMDAR minis cooperate in inhibiting dendritic protein synthesis (Sutton et al., 2004). Our results suggest that a major component of the NMDAR-mediated inhibition of local translation involves the phosphorylation (and inactivation) of eEF2. However, whereas blockade of both AMPAR and NMDAR minis enhances protein synthesis to a greater degree than NMDAR mini blockade alone, blockade of NMDAR minis fully accounts for the dephosphorylation of eEF2. These observations suggest that miniature transmission recruits an additional, as of yet unidentified mechanism for local translational suppression through AMPARs. Other studies also support a unique role for the AMPAR component of miniature synaptic transmission in mediating certain aspects of synaptic function. For example, McKinney et al. (1999) demonstrated that miniature synaptic events can maintain spine density in organotypic hippocampal slices during prolonged periods (7 days) of activity deprivation and that the AMPAR component of these events was critically important for this structural stability. Together, these observations suggest unique functional roles for the AMPAR and NMDAR components of excitatory miniature neurotransmission.

Functional Implications of Translational Control at the Level of Elongation

Although diminished rates of protein synthesis are the immediate functional consequences of lowering elongation efficiency, it has been suggested that this means of translational control serves at least two other functions. First, previous studies have demonstrated that, in some circumstances, reducing elongation efficiency can reduce translation error rates (e.g., Thompson and Karim, 1982; Abraham and Pihl, 1983). Given the metabolic cost inherent in long-range mRNA transport into dendrites at distances of hundreds of microns, translational fidelity is presumably of greater importance for local translational control in dendrites than in the soma, where translational capacity is less limiting. Thus, minis may also act to limit missense errors or premature termination of translation at individual synapses, where, based on polyribosome numbers from electron micrographs, it is likely that only a handful of mRNAs can be translated at any one time (e.g., Steward and Reeves, 1988; Ostroff et al., 2002). Second, it has been suggested that reducing elongation efficiency may favor the translation of particular mRNAs and thus serve to alter the complement of mRNAs in the actively translating pool (Walden and Thach, 1986; Scheetz et al., 2000). For example, in synaptoneurosomes prepared from superior colliculus neurons, intense NMDAR stimulation stimulates eEF2 phosphorylation, reduces global protein synthesis by 50%, and yet enhances synthesis of αCAMKII (Scheetz et al., 2000). Importantly, low concentrations of the elongation inhibitor cycloheximide also enhanced αCAMKII synthesis while depressing global translation in synaptoneurosomes, suggesting that the reduction in elongation efficiency itself can be sufficient to drive synthesis of αCAMKII (and possibly other proteins), given the appropriate context. Based on these findings, Scheetz et al. (2000) proposed that NMDAR-dependent phosphorylation of eEF2 could shift the rate-limiting step in local translation from initiation to elongation, which could select particular mRNAs for translation that are normally translated poorly. Thus, it is possible that ongoing miniature transmission alters the propensity for particular mRNAs to be locally translated, either by a mechanism similar to that proposed above or by maintaining the association of specific mRNAs with polyribosomes. It is noteworthy, however, that in our studies we find that local synthesis of a fluorescent translation reporter (which is flanked by the 5′ and 3′ untranslated regions of αCAMKII) in hippocampal neurons was suppressed by eEF2 phosphorylation driven by NMDAR minis, suggesting that the context provided by miniature synaptic transmission is not permissive for the unique mode of regulation identified by Scheetz et al. (2000). Other studies have demonstrated, for example, that strong NMDAR stimulation produces several biochemical changes that promote translation initiation (e.g., Banko et al., 2004; Kelleher et al., 2004; Gong et al., 2006), raising the question as to how these changes interact with regulation at the level of elongation. Alternatively, the inverse relationship between elongation efficiency and αCAMKII synthesis observed by Scheetz et al. (2000) might depend on a limited mRNA pool, a potential issue that we intentionally circumvent through overexpression of our reporter mRNA. In fact, mini blockade is known to broadly activate synthesis of a number of endogenous proteins (Sutton et al., 2004), suggesting that the conditions of reporter expression we use capture general changes in translational efficiency more strongly than specific regulatory mechanisms unique to αCAMKII. Nevertheless, consistent with the proposal of Scheetz et al. (2000), our results do show that the local phosphorylation of eEF2 in dendrites constrains local protein synthesis, indicating that elongation efficiency can be a limiting condition for local translational control.

Multiple Parallel Mechanisms for Coupling Activity Patterns to the Translation Machinery

A major challenge in studies of local translational control is to understand how specific regulatory mechanisms operate within the highly dynamic nature of activity within neuronal circuits. CA1 hippocampal neurons, for example, are continuously bombarded by activity from any one of the ~30,000 different inputs they receive, yet any one of these inputs may experience extended periods without AP-triggered synaptic activity. Considerable attention has been devoted to the former case, and while important progress has been made in understanding the mechanisms by which evoked activity patterns engage the

protein synthesis machinery to alter synaptic function (for reviews, see Klann and Dever, 2004; Sutton and Schuman, 2005, 2006; Pfeiffer and Huber, 2006), how these unique patterns of activity are decoded by the local translation machinery is still poorly understood. In the latter case, where evoked activity at particular inputs is low, miniature synaptic events appear to serve a local stabilizing role at synapses, preventing runaway scaling of synaptic strength during these periods of inactivity (Sutton et al., 2006). Here, we have identified eEF2 as one of the biochemical sensors that is tuned to miniature synaptic transmission, and show that it contributes to the local translational suppression conferred by miniature events. Moreover, we have shown that intrinsic AP-mediated network activity opposes the impact of miniature transmission on eEF2 phosphorylation. These results indicate that distinct modes of neurotransmission (AP-dependent versus spontaneous release) are decoded by the translational apparatus in dendrites, which implies the existence of other decoding mechanisms that act in parallel to link specific features of evoked synaptic activity (e.g., pattern, frequency) with local translational control.

EXPERIMENTAL PROCEDURES

Cell Culture and Infection

Dissociated postnatal (P1–2) rat hippocampal neuron cultures, plated at a density of 230–460 mm^2 in poly-D-lysine-coated glass-bottom petri dishes (Mattek), were prepared as previously described (Aakalu et al., 2001) and maintained for at least 21 DIV at 37°C in growth medium [Neurobasal A supplemented with B27 and Glutamax-1 (Invitrogen)] prior to use. To analyze dendritic protein synthesis, neurons were infected with a Sindbis viral vector encoding a fluorescent translation reporter (coding sequence for a myristoylated, destabilized GFP flanked by the 5′ and 3′ untranslated regions of α-CAMKII; Aakalu et al., 2001). For infection, cells were washed once with growth medium, then incubated with virus (diluted in growth medium) for 10–20 min at 37°C. Following infection, cells were washed again with growth medium, then incubated with conditioned media containing 2 μM TTX for 7–8 hr prior to imaging.

Electrophysiology

Whole-cell patch-clamp recordings were made from cultured hippocampal neurons bathed in HBS (containing 119 mM NaCl, 5 mM KCl, 2 mM $CaCl_2$, 2 mM $MgCl_2$, 30 mM glucose, and 10 mM HEPES [pH 7.4]), plus 1 μM TTX and 10 μM bicuculine, with an Axopatch 200B amplifier. Whole-cell pipette internal solutions contained 100 mM cesium gluconate, 0.2 mM EGTA, 5 mM $MgCl_2$, 2 mM adenosine triphosphate, 0.3 mM guanosine triphosphate, and 40 mM HEPES (pH 7.2), and had resistances ranging from 4–6 MΩ. Cultured neurons with a pyramidal-like morphology were voltage-clamped at −70 mV and series resistance was left uncompensated. mEPSCs were analyzed off-line using Synaptosoft mini analysis software. Statistical differences between experimental conditions were determined by ANOVA and post hoc Fisher's LSD test.

Microfluidic Experiments

Microfluidic chambers were previously developed to isolate microenvironments composed of dendritic and axonal regions (Taylor et al., 2003, 2005). These chambers consist of two parallel microfluidic channels, both connected by inlet and outlet wells. These two channels or compartments are separated by a solid barrier region with over 150 microgrooves embedded in the bottom of the connecting barrier. The dimensions of the microgrooves (7.5 μm wide, 3 μm high) allow dendrites and axons to enter, but prevent the passage of larger cell bodies. Due to the high fluidic resistance of the microgrooves, a slight volume difference between the two channels (30–50 μl) generates a pressure difference which facilitates the isolation of soluble treatments to one side. For smaller-molecular-weight molecules, which generally have larger diffusion coefficients (e.g., TTX and APV), there is some diffusion within the microgrooves after 3 hr (Figure 1B), which decreases substantially over the 900 μm barrier. Using xy scans of isolated Alexa Fluor 488 (1 μM, MW 570, 3 hr) through the microgrooves, we estimate that the concentration in the proximal 100 μm of the microgroove is <45% of the concentration in the treated side, and <3% in the distal 100 μm. Due to the small cross-sectional area of the microgrooves and the pressure gradient, we found the concentration in the adjacent compartment to be negligible.

We plated two populations of neurons on either side of the barrier, allowing processes and synaptic connections to form within the microgrooves. We applied TTX selectively to one side (the presynaptic compartment), then performed whole-cell patch-clamp recordings to examine whether APs could be selectively blocked in the treated side. Due to the pressure difference between the two compartments, there is a slight flow through the microgrooves, which generates a dilution effect in the treated side. To compensate for this, we used higher than normal concentrations of TTX (5 μM). For current-clamp recordings, we used a volume difference of 50 μl, applied TTX for 1 hr, then rinsed out the TTX and removed the poly(dimethylsiloxane) (PDMS) chamber. APs were selectively blocked for >45 min. In addition to showing that we can selectively block APs, this experiment also confirms the ability to selectively treat one compartment without influencing the other.

Neurons were infected with the reporter virus in one compartment (the postsynaptic side). Typically, 10–20 infected neurons had dendrites extending into the microgrooves, and in all cases the virus infected cells only on the virus-applied (postsynaptic) side. After 8–9.5 hr, the entire chamber was rinsed with HBS three times, then 300 μl of HBS was applied to the reporter-infected side and 250 μl of TTX (5 μM) was applied to the presynaptic side. After 1–1.5 hr, images were taken every 10 min. Three or four baseline images were taken, then the fluid was removed from the chamber, 300 μl of HBS was added to the presynaptic side, and 250 μl of APV (250 μM) was added to the postsynaptic side. Images were taken every 10 min. We estimate a concentration of APV within the microgrooves sufficient to block NMDARs (45% of 250 μM is 112.5 μM).

Western Blotting

Neurons were treated in conditioned media with TTX (2 μM) for 12 hr either alone or with CNQX (40 μM) + APV (60 μM) coincident with the last 2 hr of TTX treatment. Samples were collected in lysis buffer containing 100 mM NaCl, 10 mM $NaPO_4$, 10 mM $Na_4P_2O_7$, 10 mM lysine, 5 mM EDTA, 5 mM EGTA, 50 mM NaF, 1 mM $NaVO_3$, 1% Triton-X, 0.1% SDS, and 1 tablet Complete Mini protease inhibitor cocktail (Roche)/7 ml (pH 7.4). The samples were centrifuged at top speed in a microfuge for 15 min to remove any insoluble material, then total protein concentrations were determined by a modified Lowry assay (DC protein assay, Biorad). Equal amounts of protein for each sample (20–30 μg) were loaded and separated on 4%–15% Tris-HCl gradient gels, then transferred to polyvinylidene fluoride (PVDF) membranes. Blots were blocked with Tris-buffered saline containing 0.1% Triton-X (TBST), 5% BSA, 50 mM NaF, and 1 mM $NaVO_3$ for 60 min at room temperature (RT), and incubated with the following rabbit polyclonal primary antibodies (all from Cell Signaling Technology) for either 60 min at RT or overnight at 4°C: anti-phospho Akt (Ser473; 1:1000), anti-total Akt (1:1000), anti-phospho p42/p44 MAPK (Thr202/Tyr204; 1:2000), anti-total p42/p44 MAPK (1:2000), anti-phospho eEF2 (Thr56; 1:500), and anti-total eEF2 (1:500). After extensive washing with TBST, blots were incubated with HRP-conjugated anti-rabbit secondary antibody (1:5000; Jackson Immunoresearch) followed by

chemiluminescent detection (ECL, Amersham Biosciences). Band intensity was quantified with densitometry using NIH Image J, and the ratio of phosphorylated protein to total protein was calculated and expressed relative to the matched control sample. Statistical differences between treatment conditions and control were assessed by Chi square, whereas comparisons between TTX alone and TTX+CNQX+APV were assessed with either paired t tests (two groups) or ANOVA followed by Fisher's LSD.

Immunocytochemistry

Prior to labeling, neurons were untreated (controls) or treated with TTX (2 μM; 2.5 hr) in conditioned media either alone or with CNQX (40 μM) + APV (60 μM) or APV (60 μM) alone coincident with the last 1.5 hr of TTX treatment. Cells were then fixed on ice for 20 min with 4% paraformaldehyde/4% sucrose in PBS, permeabilized (0.1% Triton-X in PBS, 10 min), and labeled with rabbit polyclonal antibody against p-eEF2 (1:100, 60 min at RT; kindly provided by Dr. A.C. Nairn, Dept. Psychiatry, Yale University), followed by immunocytochemical detection with Alexa 488-conjugated anti-rabbit secondary antibody (1:250, 60 min at RT). Neurons were also labeled with either mouse monoclonal anti-MAP2 antibody (1:800; Sigma), followed by Alexa 546-conjugated anti-mouse secondary antibody, or with rhodamine-phalloidin (1:200, 60 min RT; Molecular Probes).

For analysis of immunocytochemistry experiments, images were obtained with Olympus IX-70 or Zeiss LSM 510 laser scanning confocal microscopes using a Plan-Apochromat 63×/1.4 oil objective. Alexa 488 and 546 were visualized by excitation with the 488 line of an argon ion laser and the 543 nm line of a HeNe laser, respectively, with emission filters of LP 505 and BP 565-615. Neurons with a pyramidal-like morphology were selected for imaging by epifluorescent visualization of MAP2 or phalloidin staining, to ensure blind sampling of p-eEF2 expression. Identical acquisition parameters were used to acquire images from each treatment condition. For analysis, the principal dendrite of each neuron was linearized using the straighten plugin for Image J, and the average nonzero pixel intensity for the p-eEF2 channel was measured for each dendrite. Data for each variable in all groups were normalized to the average value in the respective control groups (untreated or TTX alone). Statistical differences were assessed by ANOVA, followed by Fisher's LSD post hoc tests.

Live-Cell Reporter Imaging

For experiments examining synthesis of the translation reporter using bath application of eEF2 kinase inhibitors, conditioned media was replaced with HBS containing 1 μM TTX, and neurons were maintained at 37°C for 1.5–2 hr prior to imaging and throughout the experiment. All neurons chosen for experiments had a pyramidal-like morphology with one or two major dendrites emerging from the soma. After a baseline image was acquired, neurons were immediately challenged with rottlerin (5 μM), NH125 (10 μM), or 0.05% DMSO (the vehicle for both rottlerin and NH125), and imaged at 30 or 60 min intervals. Unfortunately, exposures of rottlerin and NH125 >2.5 hr were found to be cytotoxic, precluding analysis of long-term effects of eEF2 kinase inhibition. Anisomycin (40 μM), when used, was applied coincident with the initial replacement of conditioned media with HBS.

All images were acquired in 0.4 μm sections, and z-series were set to span the entire neuronal volume. Image analysis was conducted on maximal intensity z-compressed image stacks. The primary dendrite from each cell was linearized using NIH Image J, and fluorescence intensity was measured as a function of both time and distance from the cell soma. The dendritic compartment was divided into proximal and distal domains, defined by distances of less or greater than, respectively, 125 μm from the soma. Comparable changes in both proximal and distal domains were observed in these experiments, so only the data from the distal dendritic compartment is presented.

Statistical differences in reporter expression (relative to baseline) between groups were assessed by ANOVA and Fisher's LSD post hoc tests.

Local Perfusion

All local perfusion experiments were performed with an Olympus IX-70 confocal laser scanning microscope using Plan-Apochromat 40×/0.95 air or 40×/1.0 oil objectives. The delivery micropipette was pulled as a typical whole-cell recording pipette with an aperture of ~0.5 μm. The area of dendrite targeted for local perfusion was controlled by a suction pipette, which was used to draw the treatment solution across one or more dendrites and to remove the perfusate from the bath. Alexa 568 hydrazide (1 μg/ml) was included in the perfusate to visualize the affected area. The 568 nm line of a krypton ion laser was used to visualize Alexa 568 fluorescence (emitted light collected above 600 nm) and to collect differential interference contrast (DIC) images. GFP and Alexa 488 (for p-eEF2 labeling) were excited with the 488 nm line of an argon ion laser, and emitted light was collected between 510 and 550 nm. In all local perfusion experiments, the bath was maintained at 37°C and continuously perfused at 1.5 ml/min with HBS containing 1 μM TTX and other agents as indicated.

For analysis, the size of the treated area was determined in each linearized dendrite based on Alexa 568 fluorescence integrated across all images (typically 6–10) taken during local perfusion. Adjacent nonoverlapping dendritic segments, 25 μm in length, proximal (i.e., toward the cell soma) and distal to the treated area were assigned negative and positive values, respectively.

For experiments examining local regulation of p-eEF2 expression, cells were immediately fixed following local perfusion, and processed for immunostaining as described above. Analysis of p-eEF2 expression in local perfusion experiments was performed on maximal intensity z-compressed image stacks. The average nonzero pixel intensity for the entire length of the dendrite, excluding the treated area, was used to normalize p-eEF2 intensity and was assigned a value of 1. The intensity of p-eEF2 immunofluorescence was then computed for the treated and all untreated dendritic segments and expressed relative to the average nontreated value. Statistical differences in normalized p-eEF2 staining between segments were assessed by ANOVA and Fisher's LSD post hoc tests.

For experiments examining local synthesis of the translation reporter during local perfusion, reporter expression was determined from maximal intensity z-compressed stacks. Prior to local perfusion, a baseline series of images was acquired to determine the pre-existing trajectory of reporter expression dynamics in both the treated area and untreated areas of dendrites. Reporter expression in all dendritic segments was expressed relative to a baseline image taken 20–40 min prior to local perfusion. The change at each time point for each dendritic segment, excluding the treated area, was averaged and assigned a value of 1 to normalize the change in reporter expression based on the trajectory of the dendrite as a whole. Statistical differences in normalized reporter expression between segments were assessed by ANOVA and Fisher's LSD post hoc tests.

Supplemental Data

The Supplemental Data for this article can be found online at http://www.neuron.org/cgi/content/full/55/4/648/DC1/.

ACKNOWLEDGMENTS

We thank H. Weld and L. Chen for making beautiful cultured hippocampal neurons, A. Nairn for kindly providing the p-eEF2 antibody used for our immunocytochemistry experiments and for helpful discussions, and G. Laurent for solving an experimental conundrum. This work was supported by the Damon Runyon Cancer Research Foundation (M.A.S.) and the NIH (E.M.S.). E.M.S. is an investigator of HHMI.

Received: November 3, 2006
Revised: June 19, 2007
Accepted: July 25, 2007
Published: August 15, 2007

REFERENCES

Aakalu, G., Smith, W.B., Jiang, C., Nguyen, N., and Schuman, E.M. (2001). Dynamic visualization of dendritic protein synthesis in hippocampal neurons. Neuron *30*, 489–502.

Abraham, A.K., and Pihl, A. (1983). Effect of protein synthesis inhibitors on the fidelity of translation in eukaryotic systems. Biochim. Biophys. Acta *741*, 197–203.

Arora, S., Yang, J.M., Kinzy, T.G., Utsumi, R., Okamoto, T., Kitayama, T., Ortiz, P.A., and Hait, W.N. (2003). Identification and characterization of an inhibitor of eukaryotic elongation factor 2 kinase against human cancer cell lines. Cancer Res. *63*, 6894–6899.

Ashton, A.C., Volynski, K.E., Lelianova, V.G., Orlova, E.V., Van Renterghem, C., Canepari, M., Seagar, M., and Ushkaryov, Y.A. (2001). alpha-Latrotoxin, acting via two Ca2+-depdendent pathways, triggers exocytosis of two pools of synaptic vesicles. J. Biol. Chem. *276*, 44695–44703.

Banko, J.L., Hou, L., and Klann, E. (2004). NMDA receptor activation results in PKA- and ERK-dependent Mnk1 activation and increased eIF4E phosphorylation in hippocampal area CA1. J. Neurochem. *91*, 462–470.

Barria, A., Muller, D., Derkach, V., Griffith, L.C., and Soderling, T.R. (1997). Regulatory phosphorylation of AMPA-type glutamate receptors by CAM-KII during long-term potentiation. Science *276*, 2042–2045.

Bradshaw, K.D., Emptage, N.J., and Bliss, T.V.P. (2003). A role for dendritic protein synthesis in hippocampal late LTP. Eur. J. Neurosci. *18*, 3150–3152.

Carroll, M., Warrem, O., Fan, X., and Sossin, W.S. (2004). 5-HT stimulates eEF2 dephosphorylation in a rapamycin-sensitive manner in Aplysia neurites. J. Neurochem. *90*, 1464–1476.

Ceccarelli, B., Hurlbut, W.P., and Mauro, A. (1973). Turnover of transmitter and synaptic vesicles at the frog neuromuscular junction. J. Cell Biol. *57*, 499–524.

Chotiner, J.K., Khorasani, H., Nairn, A.C., O'Dell, T.J., and Watson, J.B. (2003). Adenylyl cyclase-dependent form of chemical long-term potentiation triggers translational regulation at the elongation step. Neuroscience *116*, 743–752.

De Koninck, P., and Schulman, H. (1998). Sensitivity of CAM kinase II to the frequency of Ca2+ oscillations. Science *279*, 227–230.

Fatt, P., and Katz, B. (1952). Spontaneous subthreshold activity at motor nerve endings. J. Physiol. *117*, 109–128.

Gong, R., Park, C.S., Abbassi, N.R., and Tang, S.J. (2006). Roles of glutamate receptors and the mammalian target of rapamycin (mTOR) signaling pathway in activity-dependent dendritic protein synthesis in hippocampal neurons. J. Biol. Chem. *281*, 18802–18815.

Gschwendt, M., Kittstein, W., and Marks, F. (1994). Elongation factor-2 kinase: effective inhibition by the novel protein kinase inhibitor rottlerin and relative insensitivity towards staurosporine. FEBS Lett. *338*, 85–88.

Holland, E.C. (2004). Regulation of translation and cancer. Cell Cycle *3*, 452–455.

Huber, K.M., Kayser, M.S., and Bear, M.F. (2000). Role for rapid dendritic protein synthesis in hippocampal mGluR-dependent long-term depression. Science *288*, 1254–1256.

Hughes, S.J., Smith, H., and Ashcroft, S.J.H. (1993). Characterization of Ca2+/calmodulin-depdendent protein kinase in rat pancreatic islets. Biochem. J. *289*, 795–800.

Kang, H., and Schuman, E.M. (1996). A requirement for local protein synthesis in neurotrophin-induced synaptic plasticity. Science *273*, 1402–1406.

Kelleher, R.J., Govindarajan, A., Jung, H.Y., Kang, H., and Tonegawa, S. (2004). Translational control by MAPK signaling in long-term synaptic plasticity and memory. Cell *116*, 467–479.

Klann, E., and Dever, T.E. (2004). Biochemical mechanisms for translational regulation in synaptic plasticity. Nat. Rev. Neurosci. *5*, 931–942.

Malinow, R., Schulman, H., and Tsien, R.W. (1989). Inhibition of postsynaptic PKC or CAMKII blocks induction but not expression of LTP. Science *245*, 862–866.

Marin, P., Nastiuk, K.L., Daniel, N., Girault, J.A., Czernick, A.J., Glowinski, J., Nairn, A.C., and Premont, J. (1997). Glutamate-dependent phosphorylation of elongation factor-2 and inhibition of protein synthesis in neurons. J. Neurosci. *17*, 3445–3454.

McKinney, R.A., Capogna, M., Durr, R., Gahwiler, B.H., and Thompson, S.M. (1999). Miniature synaptic events maintain dendritic spines via AMPA receptor activation. Nat. Neurosci. *2*, 44–49.

Mitsui, K., Brady, M., Palfrey, H.C., and Nairn, A.C. (1993). Purification and characterization of calmodulin-dependent protein kinase III from rabbit reticulocytes and rat pancreas. J. Biol. Chem. *268*, 13422–13433.

Nairn, A.C., and Palfrey, H.C. (1987). Identification of the major Mr 100,000 substrate for calmodulin-dependent protein kinase III in mammalian cells as elongation factor-2. J. Biol. Chem. *262*, 17299–17303.

Ostroff, L.E., Fiala, J.C., and Harris, K.M. (2002). Polyribosomes redistribute from dendritic shafts into spines with enlarged synapses during LTP in developing rat hippocampal slices. Neuron *35*, 535–545.

Pfeiffer, B.E., and Huber, K.M. (2006). Current advances in local protein synthesis and synaptic plasticity. J. Neurosci. *26*, 7147–7150.

Redpath, N.T., Price, N.T., Severinov, K.V., and Proud, C.G. (1993). Regulation of elongation factor-2 by multisite phosphorylation. Eur. J. Biochem. *213*, 689–699.

Ruggero, D., and Sonenberg, N. (2005). The Akt of translational control. Oncogene *24*, 7426–7434.

Ryazanov, A.G., Shestakova, E.A., and Natapov, P.G. (1988). Phosphorylation of elongation factor 2 by EF-2 kinase affects rate of translation. Nature *334*, 170–173.

Scheetz, A.J., Nairn, A.C., and Constantine-Paton, M. (2000). NMDA receptor-mediated control of protein synthesis at developing synapses. Nat. Neurosci. *3*, 211–216.

Silva, A.J., Stevens, C.F., Tonegawa, S., and Wang, Y. (1992). Deficient hippocampal long-term potentiation in alpha-calcium-calmodulin kinase II mutant mice. Science *257*, 201–206.

Steward, O., and Reeves, T.M. (1988). Protein-synthesis machinery beneath postsynaptic sites on CNS neurons: association between polyribosomes and other organelles at the synaptic site. J. Neurosci. *8*, 176–184.

Sutton, M.A., and Schuman, E.M. (2005). Local translational control in dendrites and its role in long-term synaptic plasticity. J. Neurobiol. *64*, 116–131.

Sutton, M.A., and Schuman, E.M. (2006). Dendritic protein synthesis, synaptic plasticity, and memory. Cell *127*, 49–58.

Sutton, M.A., Wall, N.R., Aakalu, G.N., and Schuman, E.M. (2004). Regulation of dendritic protein synthesis by miniature synaptic events. Science *304*, 1979–1983.

Sutton, M.A., Ito, H.T., Cressy, P., Kempf, C., Woo, J.C., and Schuman, E.M. (2006). Miniature neurotransmission stabilizes synaptic function via tonic suppression of local dendritic protein synthesis. Cell *125*, 785–799.

Taylor, A.M., Rhee, S.W., Tu, C.H., Cribbs, D.H., Cotman, C.W., and Jeon, N.L. (2003). Microfluidic Multicompartment Device for Neuroscience Research. Langmuir *19*, 1551–1556.

Taylor, A.M., Blurton-Jones, M., Rhee, S.W., Cribbs, D.H., Cotman, C.W., and Jeon, N.L. (2005). A microfluidic culture platform for CNS axonal injury, regeneration and transport. Nat. Methods *2*, 599–605.

Thompson, R.C., and Karim, A.M. (1982). The accuracy of protein biosynthesis is limited by its speed: high fidelity selection by ribosomes of aminoacyl-tRNA ternary complexes containing GTP. Proc. Natl. Acad. Sci. USA *79*, 4922–4926.

Walden, W.E., and Thach, R.E. (1986). Translational control of gene expression in a normal fibroblast. Characterization of a subclass of mRNAs with unusual kinetic properties. Biochemistry *25*, 2033–2041.

Wheeler, D.B., Randall, A., and Tsien, R.W. (1994). Roles of N-type and Q-type Ca2+ channels in supporting hippocampal synaptic transmission. Science *264*, 107–111.

Wu, G.Y., Deisseroth, K., and Tsien, R.W. (2001). Spaced stimuli stabilize MAPK pathway activation and its effects on dendritic morphology. Nat. Neurosci. *4*, 151–158.